Cross-shore suspended sediment transport under tidal currents

Andrew J. Hogg[1] and David Pritchard[2]

[1] Centre for Environmental & Geophysical Flows, School of Mathematics, University of Bristol, University Walk, Bristol BS8 1TW, United Kingdom
E-mail: a.j.hogg@bris.ac.uk

[2] BP Institute for Multiphase Flow, University of Cambridge, Madingley Rise, Madingley Road, Cambridge CB3 0EZ, United Kingdom
E-mail: david@bpi.cam.ac.uk

Abstract
The transport of sediment over an intertidal mudflat by a cross-shore tidal current is investigated analytically by formulating a mathematical model of the fluid and particulate motion. The model exploits the low gradient of the intertidal flats and is based upon a shallow-layer approximation. It is found that the sediment transport comprises advection with the mean flow, deposition and erosion, if the flow speed is sufficiently high. A key step in the analysis is the conversion of the evolution equation for the concentration field to a Lagrangian frame of reference. This permits the analytical computation of the concentration of sediment following fluid particles and enables the construction of non-trivial periodic solutions for the concentration field and sediment flux throughout the tidal cycle. It is shown that the current transports sediment on-shore; this is the process of settling lag and indicates that the cross-shore flows tend to accrete sediment on the intertidal mudflats. Furthermore it is shown that the gradient of the intertidal flat is directly related to the supply of sediment and the amplitude of the tidal current.

1. Introduction
Intertidal mudflats are extensive coastal regions that are characterised by the presence of fine cohesive sediment. They have extremely low gradients, leading to large tidal excursions and are often backed by low-lying salt marshes. Intertidal mudflats are common along the shores of north-western Europe and form an environment in which many species of wading birds are found, as well as being of considerable significance in their role defending the coastline from erosion.

Understanding the morphology of these coastal regions is a fundamental, outstanding scientific challenge. For example it is important to know how the mudflat and the associated sediment transport will be affected by changes in the tidal currents and the sediment supply due to climatic change or nearby engineering works, such as the construction of tidal barriers. Recent studies have sought to classify the morphodynamic regimes in terms of large-scale environmental processes ([1-3]). Kirby (2000) [3] concludes that the primary control on the cross-shore profile of an intertidal mudflat is the relative contributions of the surface waves and tidal currents to the sediment movement; the action of surface waves tends to develop concave profiles, which retreat over decadal timescales, whereas tidal currents lead to flats which are upwardly convex and accrete.

Quantitative modelling and measurement of intertidal flats remains in its infancy. Some extended programmes of field monitoring have been initiated, but the timescales of the measurements are as yet too short to permit robust conclusions to be drawn about the morphodynamic processes. Mathematical modelling of the flow processes have often been rather too simplified and inelegant to allow the subtle interplay of the dynamical effects to be elucidated clearly. A notable exception, however, is the analytical work of Friedrichs & Aubrey (1996) [4] in which the cross-shore profile is related to tidal range and the rate of sediment transport.

In this contribution we present some analytical advances in understanding the morphology of tidal flats. We focus solely on the role played by cross-shore tidal currents and neglect the effects of surface waves. Our results, therefore, are only directly applicable to sheltered mudflats. This work supplements earlier numerical studies of the flow and sediment transport over mudflats and within embayments ([5-8]) and reveals how patterns of particle movement are generated by harmonic tidal flows. In particular we can use this analysis to gain insight into the process of settling lag and into how the gradient of the flat is related to the sediment supply. We also develop the use of Lagrangian frames of reference for following the evolution of the concentration of suspended sediment within unsteady flows.

The paper is structured as follows. In §2 we formulate the mathematical model for the fluid motion and sediment transport. We recast the flow into dimensionless variables and identify the outstanding dimensionless parameters that govern the motion. We then introduce a Lagrangian technique for the analysis of the evolution

of the concentration field (§3). This is the key step in the mathematical analysis and provides a new method for generating non-trivial periodic solutions for the concentration field. We present some results for the distribution of suspended sediment and calculate the net flux of sediment throughout the tidal period. This yields a direct interpretation of the nature of morphodynamic equilibrium; the relationship between the gradient of the flats and the sediment supply; and the mechanism of settling lag, whereby sediment is transported from deep to shallow regions. Finally we summarise our results and draw some conclusions (§4).

2. Formulation

The geometry of the cross-shore model is shown in figure 1, noting that the vertical scale of this sketch has been substantially exaggerated. The water depth is denoted by $h(x,t)$ and the bed elevation by $z=d(x,t)$, where z and x are the vertical and horizontal coordinates, respectively. The free surface has an elevation, relative to an arbitrary datum, given by $\eta(x,t)$ and this generates a velocity field U with instantaneous shoreline position $x_{sh}(t)$. The flow erodes, advects and deposits suspended sedimentary particles with concentration C per unit mass. It is assumed that C is sufficiently small so that it does not affect significantly the bulk density of flow.
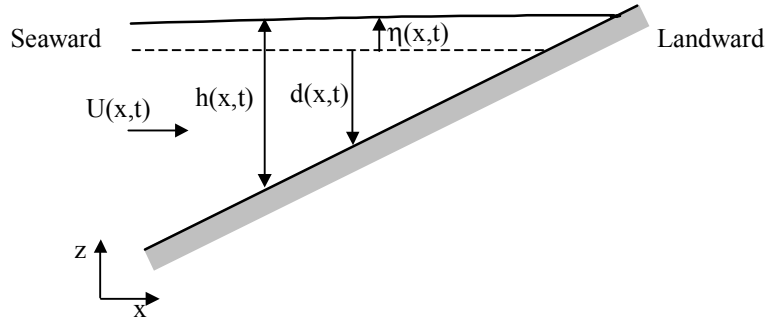

Figure 1. The configuration of the flow.

The gradient of the mudflat is small, typically of order 10^{-2} or smaller [2]. Thus it is possible to employ a shallow-water model for the motion on the assumption that the vertical accelerations are negligible and the excess pressure adopts a hydrostatic distribution given by

$$p = \rho g(h-z),\tag{1}$$

where ρ and g are the density of the fluid and the acceleration due to gravity, respectively. On the assumption that the velocity is vertically uniform, mass conservation is given by

$$\frac{\partial h}{\partial t} + \frac{\partial}{\partial x}(hU) = 0.\tag{2}$$

The streamwise momentum equation expresses a balance between inertia, hydrostatic pressure gradient, gravitational acceleration and basal drag ($\tau_b = \rho C_D U^2$) and is given by

$$\frac{\partial}{\partial t}(Uh) + \frac{\partial}{\partial x}(U^2 h) + \frac{\partial}{\partial x}\left(\tfrac{1}{2}gh^2\right) = gh\frac{\partial d}{\partial x} - C_D U^2.\tag{3}$$

Finally the suspended sediment transport is modelled on the assumption that there is sufficient fluid turbulence to maintain a vertically uniform distribution. This yields an evolution equation given by

$$\frac{\partial}{\partial t}(hC) + \frac{\partial}{\partial x}(hUC) = q_e - q_d.\tag{4}$$

In this expression horizontal diffusion has been neglected on the assumption that advection plays a more significant role and the erosion and deposition fluxes are denoted q_e and q_d, respectively. There is considerable uncertainty regarding the functional forms of q_e and q_d. Our methods, general results and conclusions are not highly dependent upon the precise relationships employed between these particulate fluxes and the other dependent variables and are robust to a wide range of different formulations [9]. However to complete our model of the motion we choose the following relationships. The erosive flux, q_e, is given by

$$q_e = m_e\left(\frac{U}{U_e^2} - 1\right) \text{ for } U > U_e; \quad \text{and } q_e = 0 \text{ for } U < U_e,\tag{5}$$

where m_e is a dimensional constant and U_e is the velocity below which no erosion occurs. This follows the model developed by Patheniades (1965) [10] for the transport of cohesive sediment and embodies the key feature that erosion does not commence until the velocity (shear stress) exceeds a critical value. For deposition, we employ

$$q_d = w_s C,\tag{6}$$

so that this settling flux is independent of the flow speed and proportional to the local concentration and the settling velocity of the suspended sediment (w_s). This model is consistent with a vertically well-mixed suspension that settles out of the flow to the underlying boundary. It could be generalised to include a critical velocity above which no deposition occurs [9]. Such a model represents the break up of mud flocs to their constituent particles at high flow speeds and turbulent intensities, which then settle considerably more slowly. In this paper we neglect such an effect.

The flow is driven by the harmonic oscillation of the elevation of the free surface far from the shoreline ($x \rightarrow -\infty$) of the form $\eta = \eta_0 \sin(2\omega t)/2$, where $\eta_0/2$ is the amplitude of the oscillation and ω is the angular frequency.

2.1 *Dimensionless variables*

We now recast the governing equations into dimensionless form using the following length, time and concentration scales. First, time-scales are rendered dimensionless with respect to $1/\omega$. Vertical lengths, namely h, d & η, are non-dimensionalised with respect to η_0, while horizontal distances are scaled by L_x, which remains as yet unspecified. Indeed, elucidating the magnitude of the gradient of the flat, η_0/L_x, remains one of the objectives of this study. Together these scales imply that the streamwise velocity, U, is non-dimensionalised with respect to ωL_x. Finally a suitable scale for the sediment concentration is given by m_e/w_s. This leads to the following dimensionless equations in which all the variables have been replaced by their dimensionless counterparts

$$\frac{\partial h}{\partial t} + \frac{\partial}{\partial x}(Uh) = 0,$$
$$\frac{\partial U}{\partial t} + U\frac{\partial U}{\partial x} = -\frac{1}{F^2}\frac{\partial}{\partial x}(h-d) - \frac{K|U|U}{h},$$
$$\frac{\partial C}{\partial t} + U\frac{\partial C}{\partial x} = \frac{E}{h}\left[\begin{cases} U^2/U_c^2 - 1, & U > U_c \\ 0, & U < U_c \end{cases} - C\right].$$

(7)

In these equations the residual dimensionless parameters are the Froude number, $F = \omega L_x/[gh_0]^{1/2}$; the drag coefficient, $K = C_D L_x/\eta_0$; the bed exchange rate, $E = w_s/[\eta_0\omega]$; and the critical velocity for erosion, $U_c = U_e/[\omega L_x]$. The bed exchange parameter and the threshold for erosion are expected to be of order unity; if they are not of this order then either the advective transport of suspended sediment is very rapid and adjusts immediately to local conditions, or it is negligible. The dimensionless drag coefficient is of order unity and Froude number is small. Thus away from the shoreline the momentum equation reduces to 'pumping' flow given by

$$\frac{1}{F^2}\frac{\partial}{\partial x}(h-d) = 0.$$

(8)

This means that the surface elevation is spatially uniform $\eta(x,t) \equiv \eta(t)$ and is equal to the far-field value. Although the effects of drag may become important in a small region close to the shoreline as the flow depth itself becomes small, in this study we will neglect drag and assume that this pumping flow description may used throughout the entire domain. The expression for mass conservation then implies that

$$U = \frac{d\eta}{dt}\frac{(x_{sh}-x)}{h}.$$

(9)

In the analysis of our results we will be concerned with the equilibrium cross-shore profiles. Thus $d \equiv d(x)$ and there is no feedback between the particulate motion and flow. We will also study the dimensionless, instantaneous sediment flux $q = CUh$ and the net flux over t tidal cycle, given by

$$Q(x) = \int_0^{2\pi/\omega} q(x,t)\, dt.$$

(10)

3. Linear tidal flat

We now investigate the solution to these reduced governing equations over an intertidal mudflat of constant gradient, given in dimensionless variables by $d(x) = -x$. Under an harmonic tidal current, $\eta = \sin(2t)/2$, this implies that the shoreline position is given by $x_{sh}(t) = \sin(2t)/2$. Thus the velocity field, U, is spatially uniform and given by $U = \cos(2t)$. The period of this tidal current is π; high-water and low-water slack occur at $t = \pi/4$ and $t = 3\pi/4$, respectively (see figure 2).

A Lagrangian fluid element at a position $x_L(t)$ is advected by the fluid velocity. Thus its velocity is given by

$$\frac{dx_L}{dt} = \cos(2t).$$

(11)

This may be readily integrated to give $x_L(t) = x_0 + \sin(2t)/2$, where x_0 (<0) represents the initial position of the fluid element and labels its subsequent motion. The depth of fluid following this Lagrangian position is constant and is given by $h_L = d + \eta = -x_0$. The reason for pursuing this Lagrangian solution is that the evolution of the

concentration field is substantially simplified. Denoting the concentration field following these Lagrangian fluid paths by $C_L(t)$, the governing equation becomes

$$\frac{dC_L}{dt} = \frac{E}{h_L}(q_e - C_L) \quad \text{on} \quad \frac{dx_L}{dt} = \cos(2t) \,. \tag{12}$$

During the tidal cycle we find that there are periods of erosion and deposition and periods within which the velocity field falls below the critical threshold for erosion and so there is only deposition (see figure 2).
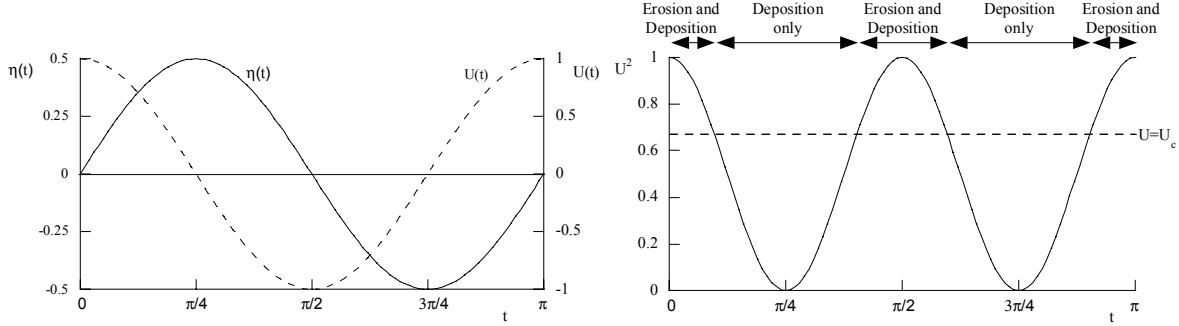

Figure 2. The tidal elevation $\eta(t)$ and the velocity $U(t)$ as functions of time. Also plotted is $U^2(t)$, showing the periods during which erosion and deposition occurs along with the periods with deposition only.

Denoting the time $t_e = \cos^{-1}(U_c)/2$, we find that there is erosion and deposition for $\pi/2 - t_e < t < \pi/2 + t_e$ and $\pi - t_e < t < \pi + t_e$ and deposition only for $t_e < t < \pi/2 - t_e$ and $\pi/2 + t_e < t < \pi - t_e$. We solve the differential equation for the concentration field C_L following Lagrangian fluid paths and demand that it is periodic. Note that since the erosive flux is proportional to U^2, it is sufficient to construct the solution during the period $t_e < t < \pi/2 + t_e$ and then simply extend the solution to the second half of the tidal cycle. In doing this we naturally generate a periodic solution; importantly, we have not imposed a far-field concentration.

We illustrate this calculation by setting $E=1$ and $U_c = 1/\sqrt{2}$, so that $t_e = \pi/8$. Thus we find that

$$C_L = \frac{-4x_0}{(1+16x_0^2)} \frac{\exp[(t - \pi/8)/x_0]}{1 - \exp[\pi/(4x_0)]} \quad \text{for } \pi/8 < t < 3\pi/8 \,, \tag{13}$$

$$C_L = \frac{\cos(4t) - 4x_0\sin(4t)}{(1+16x_0^2)} + \frac{\exp[(t-3\pi/8)/x_0]}{(1+16x_0^2)}\left(\frac{1}{1 - \exp[\pi/(4x_0)]}\right) \quad \text{for } 3\pi/8 < t < 5\pi/8 \,. \tag{14}$$

These may be converted to Eulerian concentrations by substituting $x_0 = x - \sin(2t)/2$ and recalling that $x_0 < 0$. We plot the concentration fields in figure 3a,b and observe that during the deposition only phase the concentration at the shoreline vanishes, while during the phases with both erosion and deposition it is greater than zero. This may be readily explained from the evolution equation (12). At the shoreline the height vanishes $h_L \to 0$ and so this requires that $q_e - C_L \to 0$. Thus during the phase with deposition only we must find that $C_L \to 0$, while during motion with both erosion and deposition we find that $C_L \to 2\sin^2(2t) - 1$ (when $U_c = 1/\sqrt{2}$ and $E=1$).
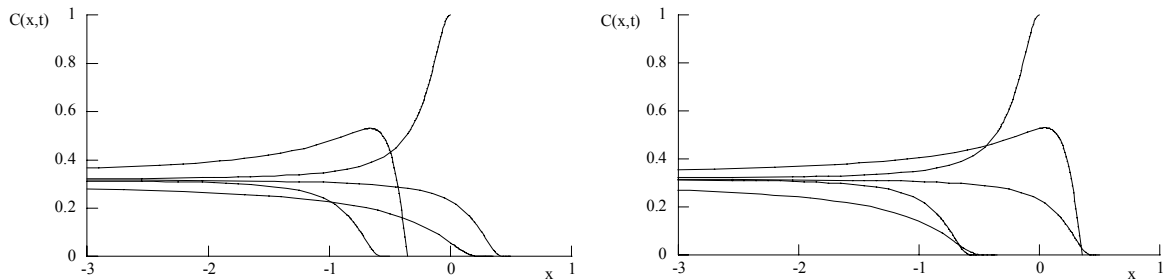

Figure 3a,b. The concentration field, $C(x,t)$, as a function of x at temporal intervals of $\pi/8$. Figure (a) shows the concentration profiles between high-water ($t=\pi/8$) and low-water ($t=5\pi/8$); figure (b) shows the concentration profiles between low-water ($t=5\pi/8$) and high-water ($t=9\pi/8$). In this plot $U_c = 1/\sqrt{2}$ and $E=1$.

The concentration within the flow attains a constant value in the far field ($x \to -\infty$). This may be readily calculated by evaluating the limit $x_0 \to -\infty$; in this case we find that $C_L \to C_\infty \equiv 1/\pi$. However there is a more

general method for calculating this far-field concentration, based on balancing the erosion and deposition over the tidal period when $h_L \rightarrow \infty$. Thus we find that

$$\int_0^\pi q_e(U)\,dt = \int_0^\pi C\,dt , \tag{15}$$

which yields

$$C_\infty = \frac{\left(1 - 2U_c^2\right)\cos^{-1} U_c + \left(1 - U_c^2\right)^{1/2} U_c}{\pi U_c^2} \tag{16}$$

We note that $C_\infty = 1/\pi$ when $U_c = 1/\sqrt{2}$ and that this equation is not defined when $U_C > 1$; this corresponds to a threshold velocity in excess of that attained by the tidal current and so no erosion occurs.
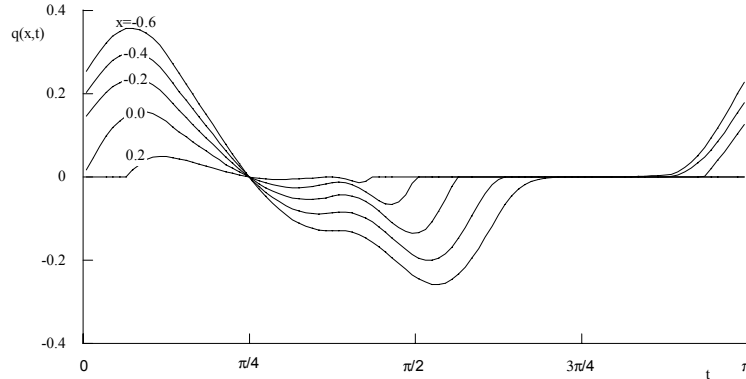

Figure 4. The flux of suspended sediment, q(x,t)=CUh, as a function of time at various positions across the intertidal flat. In this plot $U_c = 1/\sqrt{2}$ and E=1.

Using the Lagrangian expressions we find periodic solutions for the flux of suspended sediment at fixed locations across the flat. These periodic solutions are non-trivial; some examples are plotted in figure 4. They are asymmetric, with larger magnitude fluxes occurring for shorter periods during the on-shore flow. However this asymmetry diminishes as the distance from the shoreline increases. Finally we evaluate the net flux during the tidal cycle, Q(x). We find that this is small; it is an order of magnitude smaller than the instantaneous fluxes and emerges as the difference between the more substantial onshore and offshore transport. Furthermore it is positive across the entire flat, indicating that sediment is transported from deep to shallow water. Thus a linear flat will tend to develop an upwardly convex profile and will prograde.
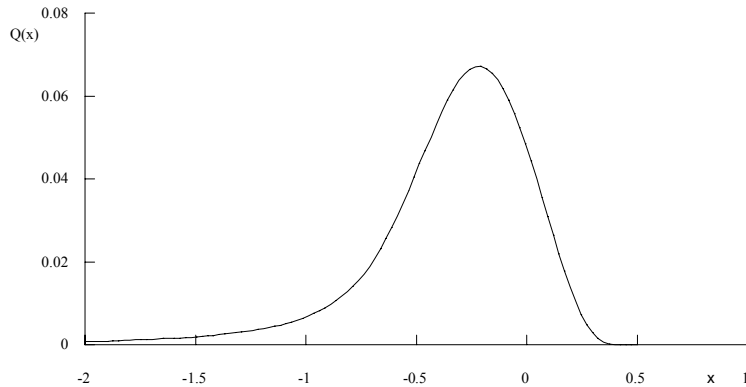

Figure 5. The net flux transport during the tidal cycle, Q(x), as a function of position. In this plot $U_c = 1/\sqrt{2}$ and E=1.

4. Discussion, Summary and Conclusions

This analysis has developed a relationship between the dimensionless threshold velocity and the scaled far-field concentration of sediment (see equation (16)). This may be used to reveal a relationship between the gradient of the flat, η_0/L_x, the dimensionless far-field concentration of sediment C_∞ and the critical velocity for erosion relative to the velocity of the tidal current, $U_e\omega/\eta_0$. Thus given a far-field concentration of sediment, such as the supply of sediment from an estuary far from the shoreline of the mudflat, and given properties of the sediment in suspension and the amplitude and frequency of the tidal current, it is possible to predict the gradient of the intertidal flat. In figure 6 we plot some contours of this function, noting that the gradient is only relatively weakly dependent on the far-field concentration.
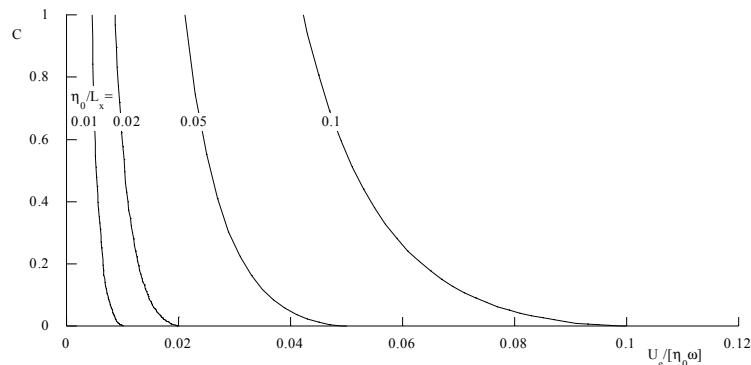
Figure 6. Contours of the gradient of the intertidal flat (η_0/L_x) as a function of the far-field concentration C_∞ and the magnitude of the threshold velocity for erosion relative to the tidal amplitude and frequency $U_e/[\eta_0\omega]$.

This calculation has also shown that the tidal current leads to a net on-shore flux of suspended sediment. This is a manifestation of the phenomenon known as settling lag [9]. In this study erosion starts at the same time across the entire flat because the velocity field is independent of the spatial coordinate. Having been eroded sediment is advected with the flow and then settles out of suspension. The dimensionless timescale of settling is proportional to the depth of the fluid element, h_L (see equation (12)). During the onshore flow, sedimentary particles are picked up and moved landwards. During the offshore motion, the same particles may be picked up but they settle out of suspension before they return to their original position because they were entrained into a shallower depth of the fluid and so the timescale for settling is shorter. By this means pumping flow over a linear flat always produces an on-shore flux of sediment as shown in figure 5.

Although the calculation here has been made for a simple geometry and flow, it is possible to apply the same techniques and analysis to more complicated scenarios. In each of the following studies, the use of a Lagrangian frame of reference permits the analytical construction of non-trivial, periodic, concentration fields that may then be used to investigate net sediment fluxes during the tidal cycle. These include pumping flow over a curved intertidal flat [9]; sediment transport by infragravity, surface waves [11]; and particulate distributions under sloshing motions within enclosed basins [12].

References
[1] Kirby, R., Effects of sea-level rise on muddy coastal margins, in *Dynamics and Exchanges in Estuaries and the Coastal Zone, Coastal Estuarine Stud.*, 40, edited by D. Prandle, AGU, Washington, D. C., (1992).
[2] Dyer, K. R., M. C. Christie, and E. W. Wright, The classification of intertidal mudflats, Cont. Shelf Res., **20**, 1039 – 1060, (2000)
[3] Kirby, R., Practical implications of tidal flat shape, Cont. Shelf Res., **20**, 1061 – 1077, (2000)
[4] Friedrichs, C. T., and D. G. Aubrey, Uniform bottom shear stress and the morphological equilibrium hypsometry of intertidal flats, in *Mixing in Estuaries and Coastal Seas, Coastal Estuarine Stud.*, **50**, edited by C. Pattiaratchi, AGU, Washington, D. C., (1996).
[5] Roberts, W., P. Le Hir, and R. J. S. Whitehouse, Investigation using simple mathematical models of the effect of tidal currents and waves on the profile shape of intertidal mudflats, Cont. Shelf Res., **20**, 1079 – 1097, (2000).
[6] Le Hir, P., *et al.*, Characterization of intertidal flat hydrodynamics, Cont. Shelf Res., **20**, 433 – 459, (2000).
[7] Pritchard, D., A. J. Hogg, and W. Roberts, Morphological modelling of intertidal mudflats: The role of cross-shore tidal currents, Cont. Shelf Res., **22**, 1887 – 1895, (2002).
[8] Schuttelaars, H. M., and H. E. de Swart, Initial formation of channels and shoals in a short tidal embayment, J. Fluid Mech., **386**, 15– 42, (1999).
[9] Pritchard, D. and A.J. Hogg, Cross-shore sediment transport and the equilibrium morphology of mudflats under tidal currents, J. Geophys. Res. **108**, 3313-3328, (2003).
[10] Partheniades, E., Erosion and deposition of cohesive soils, J. Hydraul. Eng., **91**, 105 – 139, (1965).
[11] Pritchard, D. and A.J. Hogg 2003 On fine sediment transport by long waves in the swash zone of a plane beach. J. Fluid Mech. **493**, 255-275, (2003).
[12] Pritchard, D. and A.J. Hogg Suspended sediment transport under seiches in circular and elliptical basins. Coastal Engineering 4**9**, 43-70, (2003).